FISEVIER

Contents lists available at ScienceDirect

Journal of the Mechanical Behavior of Biomedical Materials

journal homepage: www.elsevier.com/locate/jmbbm



Ultraviolet light degrades the mechanical and structural properties of human stratum corneum



Zachary W. Lipsky, Guy K. German*

Department of Biomedical Engineering, Binghamton University, 4400 Vestal Parkway East, Binghamton, NY 13902, USA

ARTICLE INFO

Keywords: Stratum corneum Ultraviolet light Photoageing Fracture Desmoglein 1

ABSTRACT

Prolonged exposure of human skin to sunlight causes photodamage, which induces the early onset of wrinkles and increased tissue fragility. While solar ultraviolet (UV) light is considered to have the most damaging effect, the UV range that is most harmful remains a topic of significant debate. In this study, we take a first step towards elucidating biomechanical photoageing effects by quantifying how exposure to different UV ranges and dosages impacts the mechanical and structural properties of human stratum corneum (SC), the most superficial skin layer. Mechanical testing reveals that irradiation of isolated human SC to UVA (365 nm), UVB (302 nm), or UVC (265 nm) light with dosages of up to 4000 J/cm² notably alters the elastic modulus, fracture stress, fracture strain, and work of fracture. For equivalent incident dosages, UVC degrades SC the greatest. However, upon discounting reflected and transmitted components of the incident light, a generalized scaling law relating the photonic energy absorbed by the SC to the energy cost of tissue fracture emerges. This relationship indicates that no one UV range is more damaging than another. Rather, the magnitude of absorbed UV energy governs the degradation of tissue mechanical integrity. Subsequent structural studies are performed to elucidate the cause of this mechanical degradation. UV absorption scales with the spatial dispersion of desmoglein 1 (Dsg 1), a component of corneocyte cell-cell junctions, away from intercellular sites. Combining both scaling laws, we establish a mechanical-structural model capable of predicting UV induced tissue mechanical integrity from Dsg 1 dispersion.

1. Introduction

Solar radiation is comprised of wavelengths ranging between 220 (ultraviolet (UV)) and 3200 nm (infrared) (Valley, 1965). Due to its greater photon energy, the impact of UV radiation on skin is the most commonly examined, however studies have explored the effects of both visible and infrared radiation (Cho et al., 2009; Kollias and Baqer, 1984; Lee et al., 2006). UV light exposure has been linked with numerous health benefits such as increased vitamin D production and phototherapy of skin conditions such as eczema (Moan et al., 2008; Reynolds et al., 2001). However, the health risks of UV overexposure are far more pervasive. UV exposure is associated with accelerated skin ageing (Panich et al., 2016), sunburn (D'Orazio et al., 2013), and the promotion of skin cancers such as basel cell carcinomas, squamous cell carcinomas, and malignant melanomas (Böni et al., 2002). UV induced skin damage can be directly caused by DNA absorption of UV light, resulting in the formation of photolesions such as cyclobutane

pyrimidine dimers or (6,4) photoproducts (Besaratinia et al., 2011; D'Orazio et al., 2013; Jiang et al., 2009; Pfeifer, 1997; Pfeifer and Besaratinia, 2012), or indirectly through the generation of reactive oxygen species, which create oxidative stresses that damage DNA, proteins, and lipids (Brem et al., 2017; D'Orazio et al., 2013; Schuch et al., 2017). The range of UV light exposure can also influence the method and level of skin damage (Besaratinia et al., 2011).

UV light is broken up into four distinct ranges: UVA (315–400 nm), UVB (280–315 nm), UVC (200–280 nm) and vacuum-UV (100–200 nm). Sunlight is comprised only of UVA and UVB light; UVC and vacuum-UV are fully attenuated by the atmosphere (U.S. Department of Health and Human Services, 2000). However, exposure of skin to UVC light can occur when using welding equipment, sunbeds, or working within biosafety cabinets (Dixon and Dixon, 2004; Meechan and Wilson, 2006; Zhang et al., 2012). In terms of overall damaging effects on full thickness skin, the World Health Organization defines UVC as the most damaging (World Health Organization, and

Abbreviations: UV, Ultraviolet; ROS, Reactive oxygen species; SC, Stratum corneum; RH, Relative humidity; Dsg 1, Desmoglein 1; PBS, Phosphate-buffered saline; Dsc 1, Desmocollin 1; CDSN, Corneodesmosin

^{*} Corresponding author. Binghamton University, Department of Biomedical Engineering, BI2609, 4400 Vestal Parkway East, Binghamton, NY 13902, USA. E-mail address: ggerman@binghamton.edu (G.K. German).

International Programme on Chemical Safety., 1994). However, different UV ranges do not impact skin tissue equally; UV light has wavelength-dependent penetration depths. While longer wavelength UVA can reach deep into the dermis, UVB and UVC light are primarily absorbed by the epidermis (Meinhardt et al., 2008). As such, consideration for which tissue layer is affected needs to be accounted for. Moreover, reports of skin damage from different UV light ranges is evaluated primarily from a biological standpoint. Here, damage is characterized by its impact on cellular DNA (Dong et al., 2008; Kvam and Tyrrell, 1997; Pfeifer and Besaratinia, 2012; Schuch et al., 2017; Tadokoro et al., 2003) and carcinogensis (Buckman, 1998; Chen et al., 2013; de Gruiil et al., 2001; Ziegler et al., 1994), rather than the potential for UV light to physically degrade skin integrity. While studies have explored UV light induced changes in skin elasticity (Nishimori et al., 2001; Oba and Edwards, 2006), and UVB's effect on the mechanical properties of the most superficial skin layer, the stratum corneum (SC) (Biniek et al., 2012), the relative impact of the different UV ranges on the structural and mechanical integrity of human skin remains unclear, as does the mechanism of degradation. In this study, we provide initial insight into the comparative damaging effects of different UV ranges by exploring how various UVA, UVB, and UVC light dosages change the mechanical and structural properties of human SC.

2. Materials and methods

2.1. Stratum corneum isolation

Full thickness 36 yrs. female breast skin specimens (n = 3) were received from Yale Pathology Tissue Services (New Haven, CT) within 24 h. of elective surgery. Breast tissue was chosen because it is typically exposed only to low levels of solar UV exposure. An exempt approval (3002-13) was obtained to perform research using de-identified tissue samples pursuant to the Department of Health and Human Services (DHHS) regulations, 45 CFR 46.101:b:4. SC was isolated using a standard heat bath and trypsin technique (German et al., 2013; Kligman and Christophers, 1963; Liu and German, 2015). Once isolated, SC sheets were placed on plastic mesh (Darice, Strongsville, OH), rinsed in deionized water, and dried for 48 h. at room temperature and humidity. For uniaxial mechanical testing, SC samples were cut to a uniform $7 \times 20 \,\mathrm{mm}$ size (n = 142 total samples used for the study). For immunostaining studies, samples were cut to a uniform 6 mm diameter circle (n = 26 total samples used for the study). While full thickness skin exhibits mechanical anisotropy (Langer, 1861; Ní Annaidh et al., 2012), SC tissue exhibits isotropic mechanical properties (Koutroupi and Barbenel, 1990; Takahashi et al., 1981). As such, the orientation of SC samples cut from the isolated sheet are unimportant.

2.2. Ultraviolet irradiation

UV irradiation of SC samples was performed using a UV Lamp (8 Watt EL Series, Analytik Jena US LLC, Upland, CA) with stand. For mechanical testing, SC samples were exposed to UVC (265 nm narrowband), UVB (302 nm narrowband) or UVA (365 nm narrowband) light for periods equating to incident light dosages of 10, 100, 200, 400, 800 and 4000 J/cm². For structural studies, SC samples were exposed to UVC, UVB or UVA light for periods equating to incident light dosages of 100, 200, 400, and 800 J/cm². For samples positioned 76 mm from the light source, the average intensities of the UVA, UVB, and UVC lamp bulbs are 1.5 mW/cm², 1.6 mW/cm², and 1.8 mW/cm² respectively (Gasperini et al., 2017). To achieve equal dosages across the three UV ranges, exposure times were varied. For instance, a dosage of 10 J/cm² required an exposure time of 111 min for UVA, 104 min for UVB, and 92 min for UVC. SC samples exposed only to ambient UV light were used for controls.

2.3. Mechanical characterization

After UV irradiation, samples were equilibrated for 24 h. to either 25 or 100% relative humidity (RH) before testing. Equilibration to low or high RH conditions was achieved by placing specimens respectively in an airtight container filled with desiccant (Drierite 10-2 mesh, W.A. Hammond Drierite Company, Xenia, OH) or a hydration cabinet (F42072-1000, Secador, Wayne, NJ) with a base filled with deionized water. In both cases, RH conditions were monitored throughout the equilibration period using a hygrometer with probe (445815, Extech Instruments, Nashua, NH)). After equilibration, the mechanical properties of samples were evaluated using a uniaxial tensometer (UStretch, CellScale, Waterloo, ON, Canada) equipped with a 4.4 N load cell. The ends of each SC sample were taped (General-Purpose Laboratory Labeling Tape, VWR, Radnor, PA) to prevent slippage of the sample in the tensometer grips, leaving an exposed area of 7×10 mm. Individual SC samples were mounted into opposing tensometer grips, initially separated by 10 mm. Samples were strained until rupture at a constant strain rate of 0.012 s⁻¹; similar to rates used in previous mechanical studies of skin (Ní Annaidh et al., 2012). Tensile forces and grip separation were recorded at a frequency of 5 Hz. After mechanical testing, the average thickness of the ruptured SC sample was quantified with optical microscopy using an Eclipse Ti-U inverted microscope (Nikon, Melville, NY) with 40X oil objective lens (Nikon Plan UW, Nikon, Melville, NY). Optical thickness measurements were taken a distance from the crack interface to prevent measuring reduced thicknesses arising from plastic deformation. Combinations of sample dimensions, and recorded force-displacement data were then used to derive engineering stress-strain curves, from which the average elastic modulus, fracture stress, fracture strain and work of fracture were extracted $(3 \le n \le 9)$ independent samples for each UV range, dosage, and humidity).

2.4. Desmoglein 1 dispersion analysis

Irradiated and control samples (3 mm diameter circle, n = 2 for each condition) were first incubated with an anti-demoglein 1 (Dsg 1) mouse monoclonal antibody (651110, Progen, Heidelberg, Germany) at a 1:500 ratio antibody to phosphate-buffered saline (PBS, P5368, Sigma, St Louis, MO) at 4 °C overnight (Naoe et al., 2010; Oyama et al., 2010). Samples were then washed three times with PBS before being incubated in a 1:200 ratio of Alexa-Fluor 488 labeled goat anti-mouse IgG antibody (A-11029, Introgen, Carlsbad, CA) to PBS for 1 h. at room temperature. Samples were then rewashed in PBS three times before being placed on a glass coverslip. Images of control and irradiated SC were recorded using a confocal microscope (Leica SP5, Wetzlar, Germany) and 63x oil objective lens, with numerical aperture of 1.4 and spatial resolution of 0.15 $\mu m/pixel$ (1024 imes 1024 pixels). A 488 nm wavelength laser was used to excite the SC samples. Fluorescent emissions were recorded in the range 500–540 nm. For each UV condition, a total of n = 20 intercellular junctions between corneccytes (from n = 2 independent SC samples) were identified. Intercellular junctions were considered to be located along the coinciding perimeters of adjacent corneocytes, where Dsg 1 is typically located (Yokouchi et al., 2016). Perpendicular cross sectional fluorescent intensity profiles (n = 100) were then extracted from each identified intercellular junction, spanning \pm 2.5 μm on either side of the intercellular interface. This width was sufficiently large to characterize a ~62% reduction in Dsg 1 fluorescent intensity for unirradiated controls. For each UV condition analyzed, a total n = 2000 individual profiles were normalized by peak pixel intensity and averaged (as detailed in Fig. S1 of the Supplemental Material).

2.5. Statistical analysis

All statistical analyses were performed using R (version 3.4.2). A 1-way ANOVA was used to test for statistical significance in Figs. 1 and 2,

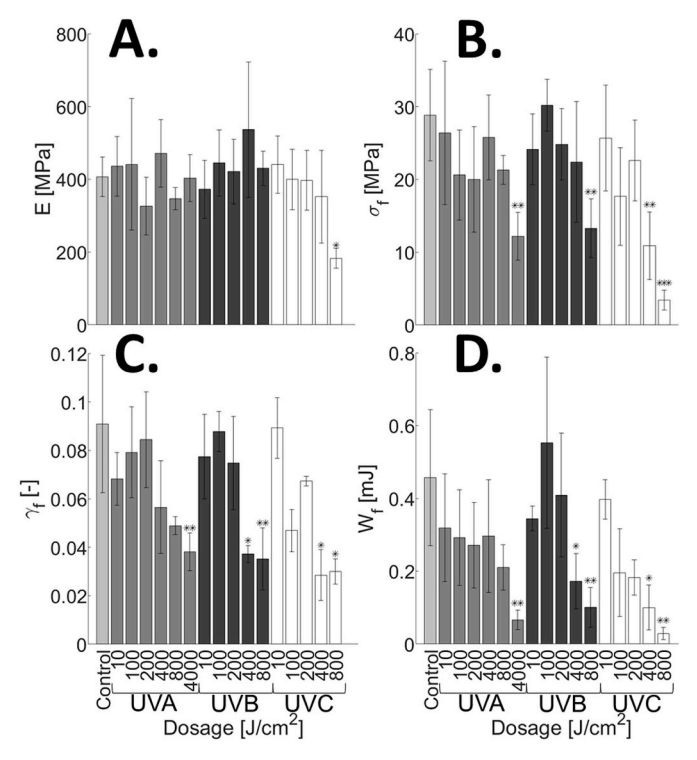


Fig. 1. UV induces changes in the mechanical properties of SC equilibrated to 25% RH. Average (A) elastic modulus, E, (B) fracture stress, σ_f , (C) fracture strain, γ_f , and (D) work of fracture, W_f for unirradiated controls (Control; light grey), UVA irradiated samples (dosage range: $10-4000 \, \mathrm{J/cm^2}$; medium grey), UVB irradiated samples (dosage range: $10-800 \, \mathrm{J/cm^2}$; dark grey), and UVC irradiated samples (dosage range: $10-800 \, \mathrm{J/cm^2}$; white). Bars denote average values of $3 \le n \le 9$ individual sample measurements for each range and dosage condition. Error bars denote standard deviations.

where each UV condition (UVA, UVB, and UVC) was compared to the control. Levene's and Shapiro-Wilk's tests were respectively used to determine equality of variances and normality. Results in Fig. 1C (controls), Fig. 2A (UVA 10 and 200 J/cm²), Fig. 2B (UVB 10 J/cm²), Fig. 2C (UVB 800 J/cm², UVC 800 J/cm²), and Fig. 2D (UVB 100 J/cm², UVC 800 J/cm²) were found to exhibit non-normal distributions, but equal variances. Here a Kruskal-Wallis analysis was performed. Results in Fig. 1D (UVB), and Fig. 2B–D (UVB) were found to exhibit normal distributions, but unequal variances. Here a 1-way ANOVA with Welch correction was performed. Post-hoc analyses were performed if statistical significance levels below 5% were established. In the figures, * denotes $p \le 0.05$, ** denotes $p \le 0.01$, and *** denotes $p \le 0.001$.

3. Results and discussion

3.1. Changes in SC mechanical properties with UV irradiation

Changes in the mechanical integrity of human SC with UV light range and dosage are first assessed. Isolated human SC samples are irradiated with incident dosages of narrowband UVA (365 nm), UVB (302 nm) or UVC (265 nm) light ranging between 0 (Control) and 4000 J/cm²; the latter dosage being equivalent to approximately 8 continual days of full-spectrum solar UVA (or 361 continual days solely at 365 nm) (ASTM G173-03, 2012). UV therapy treatments for various skin diseases including vitiligo, pruritus, inflammatory dermatoses, and scleroderma can have cumulative dosages of up to 485 J/cm² for narrowband UVB (311 nm) (Kleinpenning et al., 2009; Tjioe et al., 2002; Yashar et al., 2003) and 2000 J/cm² for broadband UVA (340–400 nm) (De Rie et al., 2003; Kreuter et al., 2006; Kroft et al., 2008). Fig. 1A–D respectively show the average ($3 \le n \le 9$ samples for each UV dosage)

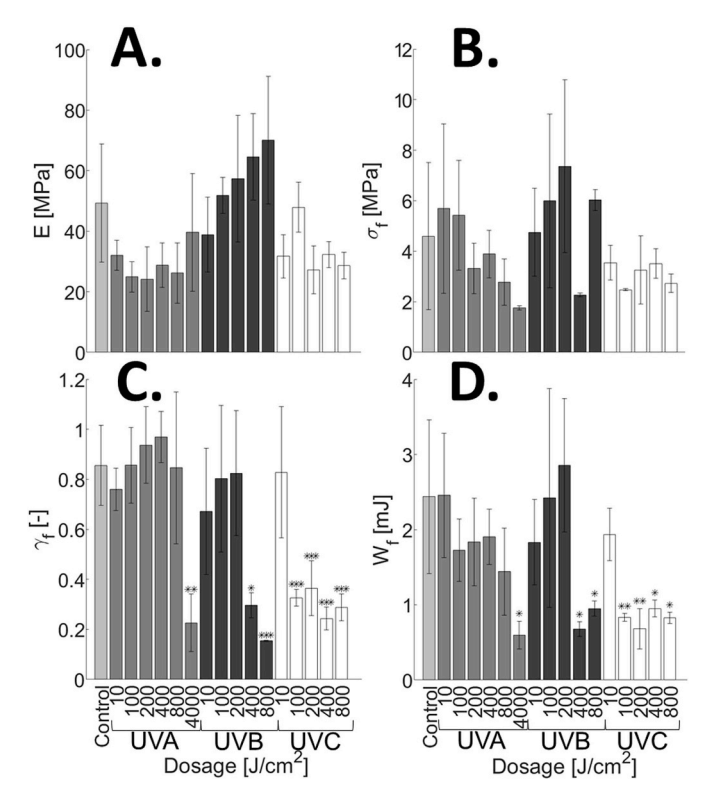


Fig. 2. UV induces changes in the mechanical properties of SC equilibrated to 100% RH. Average (A) elastic modulus, E, (B) fracture stress, σ_f , (C) fracture strain, γ_f , and (D) work of fracture, W_f for unirradiated controls (Control; light grey), UVA irradiated samples (dosage range: $10-4000 \, \text{J/cm}^2$; medium grey), UVB irradiated samples (dosage range: $10-800 \, \text{J/cm}^2$; dark grey), and UVC irradiated samples (dosage range: $10-800 \, \text{J/cm}^2$; white). Bars denote average values of $3 \le n \le 7$ individual sample measurements for each range and dosage condition. Error bars denote standard deviations.

elastic modulus, E, fracture stress, σ_f , fracture strain, γ_f , and work of fracture, W_f , of irradiated samples equilibrated for 24 h. to 25% relative humidity (RH) prior to mechanical testing. Fig. 1A highlights that no significant change in elastic modulus occurs with either UVA or UVB irradiation, however a UVC dosage of $800\,\mathrm{J/cm^2}$ induces a significant decrease in tissue stiffness, relative to controls. Fig. 1B shows that samples undergo no significant reduction in fracture stress for UVA dosages less than $4000\,\mathrm{J/cm^2}$, UVB dosages less than $800\,\mathrm{J/cm^2}$, and UVC dosages less than $400\,\mathrm{J/cm^2}$. However, dosages at or above these levels cause statistically significant decreases. Similarly, Fig. 1C and D show that significant decreases in both the fracture strain and work of fracture occur with UVA dosages of $4000\,\mathrm{J/cm^2}$, and both UVB and UVC dosages equal to or greater than $400\,\mathrm{J/cm^2}$.

Fig. 2A–D show complementary mechanical results for SC samples $(3 \le n \le 7 \text{ samples for each dosage})$ equilibrated for 24 h. to 100% RH prior to mechanical testing. In contrast to the 25% RH results in Fig. 1, Fig. 2A and B highlight that no significant change in either the elastic modulus or fracture stress occurs for any UV treatment. Reductions in sample fracture strain and work of fracture however occur with UVA and UVB dosages of 4000 J/cm² and 400-800 J/cm² respectively, as shown in Fig. 2C and D. This trend is similar to that observed for samples equilibrated to 25% RH (Fig. 1C and D), however the magnitude by which these parameters decrease is notably larger for the hydrated SC. Moreover, UVC dosages of 100 J/cm² or greater also induce statistically significant decreases. The lack of statistically significant changes in elastic modulus (Figs. 1A and 2A) with UVB irradiation, along with observed decreases in fracture strain with increasing UVB dosage (Figs. 1C and 2C) are consistent with previous studies (Biniek et al., 2012). In addition, control results at 25% and 100% RH fall

within the diverse range of previously reported human SC data at high (100%) and low (0%) RH for elastic moduli (E=5-1000 MPa) (Biniek et al., 2012; Koutroupi and Barbenel, 1990; Liu et al., 2016; Wildnauer et al., 1971; Wu et al., 2006), fracture stress ($\sigma_f=2.6-22$ MPa) (Biniek et al., 2012; Koutroupi and Barbenel, 1990; Liu et al., 2016; Wildnauer et al., 1971; Wu et al., 2006), and fracture strain ($\gamma_f=0.8-0.048$) (Biniek et al., 2012; Liu et al., 2016; Wildnauer et al., 1971).

Results in Figs. 1 and 2 appear to highlight that for equivalent incident dosages, UVC light induces the greatest loss in SC mechanical integrity, followed by UVB, then UVA. However, the incident dosage does not equate with the physical energy absorbed by the SC tissue (Bruls et al., 1984; Diffey, 1983). UV light is absorbed, reflected, and transmitted through the SC; the degree with which each of these occurs is wavelength dependent. Prior studies have shown that the percentage of incident UVA, UVB, and UVC light absorbed by the SC is 25, 48, and 71%, respectively (Diffey, 1983). Table S1 shows the energy physically absorbed by the SC for each UV range and incident dosage. We further scrutinize our data to establish whether a relationship exists between the energy absorbed by the SC, and the associated degradation in its mechanical integrity.

3.2. Scaling of absorbed UV dosage with work of fracture

Figs. 3 and 4 respectively show the work of fracture plotted against the physical energy absorbed by individual SC samples, when equilibrated to 25 and 100% RH. Both figures reveal that irrespective of the UV range used, increases in the energy absorbed by the tissue decrease the work of fracture. For each figure, a relationship between the average work of fracture, W_f , and the absorbed dosage, φ , is established by fitting the data with a nonlinear least-squares regression of the form;

$$W_f = W_0 e^{C_1 \varphi}. \tag{1}$$

Best fits were made with power-law, exponential, and linear models. The exponential model in each case provides the strongest correlation. The grey shaded region in each figure corresponds to the standard deviation about the average work of fracture at each dosage. For tissue equilibrated to 25% RH, $W_0 = 0.395 \, \mathrm{mJ}$ and $C_1 = -3.61 \times 10^{-3}$. A p-value of $p = 5 \times 10^{-4}$ for the goodness of fit supports the notion that absorbed dosage acts as a predictor of tissue mechanical integrity, with an R-squared value of 0.69. Likewise, for tissue equilibrated to 100% RH, $W_0 = 2.01 \, \mathrm{mJ}$ and $C_1 = -1.73 \times 10^{-3}$. A p-value of $p = 6 \times 10^{-3}$ is also established for the goodness of fit, with an R-squared value of 0.48. These results indicate that irrespective of the UV range used, the dosage

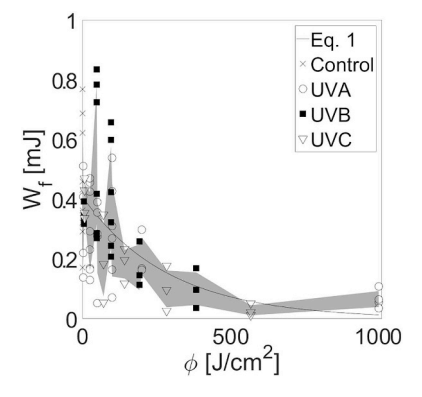


Fig. 3. Change in the work of fracture with UV energy absorbed by SC equilibrated to 25% RH. Work of fracture, W_f , of individual SC samples plotted against absorbed UV dosage, φ , for controls (cross), and samples irradiated with UVA (open circle), UVB (filled square), and UVC (open inverted triangle). An exponential least-squares best fit is represented by the solid black curve (Eq. (1), $W_0 = 0.395 \,\mathrm{mJ}$, $C_1 = -3.61 \times 10^{-3}$). The shaded region indicates the standard deviation of the data points about the mean work of fracture at each dosage.

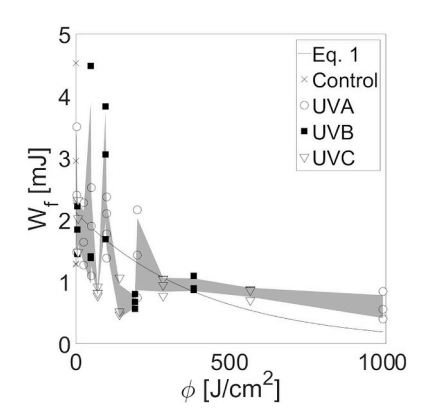


Fig. 4. Change in the work of fracture with UV energy absorbed by SC equilibrated to 100% RH. Work of fracture, W_f , of individual SC samples plotted against absorbed UV dosage, φ , for controls (cross), and samples irradiated with UVA (open circle), UVB (filled square), and UVC (open inverted triangle). An exponential least squares best fit is represented by the solid black curve (Eq. (1), $W_0 = 2.01 \, \mathrm{mJ}$, $C_1 = -1.73 \times 10^{-3}$). The shaded region indicates the standard deviation of the data points about the mean work of fracture at each dosage.

absorbed by the tissue appears to be primary driving force behind the degradation of mechanical integrity.

3.3. Dispersion of intercellular desmoglein 1 with UV irradiation

While our results clearly demonstrate a loss of tissue mechanical integrity with sufficient irradiation from all UV ranges, the underlying cause of this degradation remains unclear. Previous studies have highlighted that tissue hydration is the predominant factor in altering the mechanical properties of SC (Alonso et al., 1996; Liu et al., 2016; Papir et al., 1975; Wildnauer et al., 1971; Wu et al., 2006). Reductions in water content are associated with increases in tissue elastic modulus (Alonso et al., 1996; Liu et al., 2016; Papir et al., 1975; Wildnauer et al., 1971; Wu et al., 2006), and notable decreases in the ability of SC to plastically deform prior to rupture (Liu et al., 2016; Wildnauer et al., 1971). While reductions in plastic deformability of SC equilibrated to 100% RH do occur with UV irradiation, as demonstrated in Fig. 5, associated increases in elastic modulus are absent (Figs. 1A and 2A). Therefore, a structural change is more likely to be the primary cause of the observed SC mechanical degradation. Alterations to the corneodesmosome junctions is an attractive explanation due to its role as a major structural protein that provides intercellular cohesion (Jonca et al., 2002; Kitajima, 2015). Moreover, SC fracture has been noted to

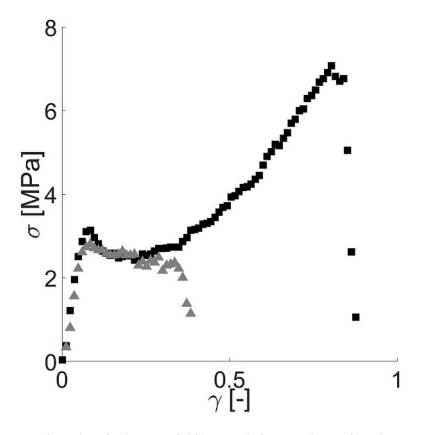


Fig. 5. Loss of SC plastic deformability with UV irradiation. Representative stress-strain plots of an unirradiated SC sample (filled squares) and a sample irradiated with 400 J/cm² of incident UVB light (filled triangle). Both samples are equilibrated to 100% RH.

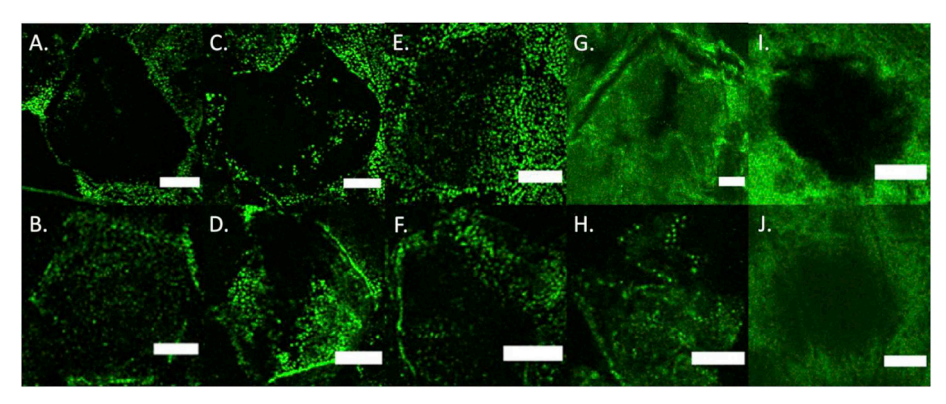


Fig. 6. Confocal images showing changes in fluorescently tagged desmoglein (Dsg 1) distributions with increasing UVB dosage. Dsg 1 fluorescent images (from n = 2 individual samples per condition) of control samples (A,B) and samples irradiated with an incident dosage of 100 J/cm^2 (C,D), 200 J/cm^2 (E,F), 400 J/cm^2 (G,H), and 800 J/cm^2 UVB (I,J). (*Scale bar*) 10 µm.

occur primarily intercellularly (Liu et al., 2016). While all components of corneodesmosomes, including desmocollin 1 (Dsc 1), corneodesmosin (CDSN) and desmoglein 1 (Dsg 1), may be affected by UV irradiation, Dsg 1 has shown the most evidence of alteration causing intercellular instability (Amagai et al., 2002; Borgoño et al., 2007; Descargues et al., 2005; Eyre and Stanley, 1987). Therefore, the impact of UV irradiation on changes to the presence and location of Dsg 1 is consequently investigated using immunostaining.

Fig. 6 shows the change in distribution of fluorescently tagged Dsg 1 in SC samples irradiated with increasing UVB exposure. Control SC samples exposed only to ambient UV in Fig. 6A and B exhibit commonly observed Dsg 1 distributions, characterized by small distinct puncta surrounding the periphery of corneocytes (Johnson et al., 2014; Naoe et al., 2010; Oyama et al., 2010). Incident UVB dosages of 100 J/cm² (Fig. 6C and D) and 200 J/cm² (Fig. 6E and F) display similar distributions. However Fig. 6G–J show that with incident UVB dosages of 400 J/cm² or greater, Dsg 1 lose their distinctive puncta morphology, and become more dispersed. Distribution changes in Dsg 1 with UVB exposure has been cited previously with organotypic cultures, but not to our knowledge with *ex vivo* human SC (Johnson et al., 2014).

The progressive dispersion of Dsg 1 is further quantified across all UV types (UVA, UVB and UVC) and dosages (0-800 J/cm²) by characterizing the average fluorescent normalized pixel intensity (NPI) profiles perpendicularly across intercellular junctions. Average NPI profiles for each UV range and dosage are established from n = 2000intercellular junction profiles (n = 2 samples; n = 10 junctions per sample; n = 100 cross sections per junction). Profiles from UVB irradiated samples are displayed in Fig. 7A-E. UVA and UVC irradiated profiles are provided in Figs. S2A-D and E-H respectively. All cross sectional profiles, irrespective of UV type and dosage, exhibit peak NPI values at or near the center of the cross sectional profile, coincident with the cell-cell interface. However, while intensity profiles exhibit a narrow peak at the cell-cell interface for UVB dosages of 200 J/cm² or less (Fig. 7A-C), consistent with dense localized puncta, greater dosages (Fig. 7D and E) exhibit notably wider peaks, indicative of dispersion. UVA and UVC irradiated samples also exhibit this trend, with profile peaks widening with UVA dosages greater than or equal to 800 J/cm² (Fig. S2D) and UVC dosages greater than or equal to 200 J/cm² (Figs. S2F-H). These results indicate that increasing dosages result in increased dispersion of desmoglein for all UV ranges. To better understand this dispersion, NPI profiles are fitted with a double gaussian

$$NPI = \frac{1}{\sigma_1 \sqrt{2\pi}} e^{-\frac{1}{2} (\frac{x}{\sigma_1})^2} + \frac{1}{\sigma_2 \sqrt{2\pi}} e^{-\frac{1}{2} (\frac{x}{\sigma_2})^2},$$
 (2)

where σ_i is the standard deviation and x denotes the lateral position across the averaged *NPI* profile (– 2.5 \leq x \leq 2.5 μ m). The best-fit model to the control treatment profile is shown as the dotted-line in

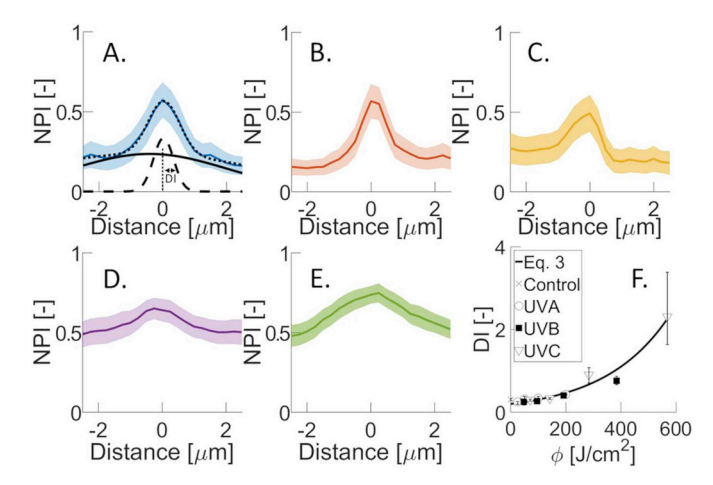


Fig. 7. Changes in averaged normalized pixel intensity (NPI) profiles across intercellular corneocyte junctions with increasing UVB dosage. (A) control samples (blue line), (B) $100 \, \mathrm{J/cm^2}$ incident dosage (red line), (C) $200 \, \mathrm{J/cm^2}$ incident dosage (yellow line), (D) $400 \, \mathrm{J/cm^2}$ incident dosage (purple line), and (E) $800 \, \mathrm{J/cm^2}$ UVB incident dosage (green line). Shaded regions correspond to the standard error about the mean curve. Eq. (2) is used to fit average NPI profiles. The black dotted line denotes the best fit to the average control NPI profile in panel A. The two individual composite gaussian distributions of Eq. (2) are also represented in this panel by black solid- and dashed-lines. The inner gaussian (black dashed-line) is used to establish the dispersion index (DI), equivalent to the standard deviation of the distribution. (F) Change in dispersion index, DI, with UVA (open circle), UVB (filled square), and UVC (open inverted triangle) energy absorbed by SC. An exponential least-squares best fit to all the data points is represented by the solid black curve. Error bars denote standard deviations.

Fig. 7A. The inner and outer gaussian components of Eq. (2) are also plotted in Fig. 7A as dashed and solid curves, respectively. We employ the standard deviation of the inner gaussian function to characterize the dispersion of desmoglein, which we denote the dispersion index, DI. Fig. 7F plots DI against the absorbed UV dosage, φ , irrespective of UV type. Similar to Figs. 3 and 4, an exponential function of the form,

$$DI = DI_0 e^{C_2 \varphi} \tag{3}$$

is found to provide the best fit to the data. For the regression, $DI_0 = 0.199$ and $C_2 = 4.27 \times 10^{-3}$. A p-value of $p = 7 \times 10^{-4}$ for the goodness of fit supports the absorbed dosage acting as a predictor of Dsg 1 distribution, with an R-squared value of 0.96.

Changes in both the average work of fracture (Figs. 3 and 4), W_f , and structural dispersion index (Fig. 7F), DI, with absorbed UV dosage, φ , exhibit exponential relationships. Combining Eqs. (1) and (3), we establish a power law expression relating structural and mechanical

parameters of the form,

$$W_f = W_0 \left(\frac{DI}{DI_0}\right)^{\alpha}. \tag{5}$$

where $\alpha = C_1/C_2$. For SC samples equilibrated to 25% RH, $\alpha = -0.845$. This structure-mechanical relationship highlights that the mechanical integrity of the SC tissue scales with near inverse proportionality to the dispersion of intercellular junction proteins away from intercellular interfaces. We restrict this model to tissue equilibrated to dry (25% RH conditions) conditions because all UV irradiation protocols were performed on dry tissue samples to minimize surface, unbound, and bound water (Vyumvuhore et al., 2013; Walkley, 1972) altering the absorption, reflection, and transmission of UV (Bruls et al., 1984; Bruls and Van Der Leun, 1984; Hoffmann et al., 2000; Kolmel et al., 1990). Moreover, SC equilibrated to a lower relative humidity is more physiologically consistent in-vivo SC tissue (20–40% RH indoors (Arundel et al., 1986); 30–80% RH outdoors (Dai, 2006)).

While a structure-mechanical relationship is established between dispersion of Dsg 1 and mechanical integrity of the SC, the mechanism by which UV radiation causes the dispersion of Dsg 1 remains unknown. Previous work has shown that SC serine proteases that hydrolyze corneodesmosome components, such as Dsg 1, exhibit increased activity with UVB exposure in cultured epidermal keratinocytes (Nin et al., 2009). Therefore, in order to explore the influence of ex vivo SC enzymes on Dsg 1 dispersion, we employ in situ zymography (Nin et al., 2009; Yamasaki et al., 2007). Fig. S3 within the supplemental material shows a significant increase in fluorescence within the SC after an incident dosage of UVB at 800 J/cm2 is applied, compared to non-irradiated tissue. This can be attributed to increased protease activity. While corneodesmosomes have also been noted to degrade with prolonged exposure to high humidity or with water incubation (Rawlings et al., 1995; Warner et al., 2003), research has shown that when ex vivo SC is incubated in water and serine protease inhibitors, SC integrity is not as greatly affected (Rawlings et al., 1995). As such, this suggests that UV light induced increases in protease activity is more likely than hydration alone to contribute to the observed structural changes in Dsg 1 within corneodesmosomes, resulting in mechanical degradation.

4. Conclusion

In this article, we quantify the impact of UV range and dosage on the mechanical and structural degradation of isolated human stratum corneum (SC). For equivalent incident dosages, UVC light causes the greatest loss in SC mechanical integrity, followed by UVB and UVA. This is due to the greater radiation energy of UVC light. However, when discounting reflected and transmitted components of the incident light, a scaling law relationship between the energy absorbed and the work of SC fracture emerges. This relationship highlights that no one UV range is more damaging than another. Rather, the amount of energy absorbed governs the loss of tissue mechanical integrity. Further structural studies reveal that desmoglein 1 (Dsg 1), a major component of corneodesmosomes, becomes dispersed with UV exposure away from intercellular sites. Upon relating the mechanical and structural models, a near inverse scaling law is revealed. This suggests that a simple immunostaining assay could therefore be employed to quantify UV induced tissue damage.

We highlight that an increase in SC protease activity from UV irradiation is likely to contribute to the observed structural changes in Dsg 1 within corneodesmosomes, resulting in mechanical degradation. While other SC components, including keratin, the cornified envelope, and lipids (Biniek et al., 2012; Fujita et al., 2007; Hirao and Takahashi, 2005; Iwai and Hirao, 2008; Lee et al., 2016; Mizutani et al., 2016; Sander et al., 2002; Thiele et al., 1999) have also been shown to exhibit structural changes with UV light exposure, SC has been noted to fracture primarily intercellularly (Liu et al., 2016), where corneodesmosomes reside. As such, corneodesmosomes that play a major contributor

of cell-cell adhesion (Jonca et al., 2002; Kitajima, 2015) are more likely to play a dominant role in defining the mechanical strength of the tissue compared to other SC components. In addition, although out-of-plane changes in the mechanical properties of SC with UV irradiation may occur, the mechanistic cause of this is unlikely to differ from in-plane testing completed here. Similar to in-plane studies, out-of-plane studies (Wu et al., 2006) have also shown that SC fracture occurs primarily intercellularly. Furthermore, the 10-20 layers of corneocytes (Cork et al., 2006; Silva et al., 2007) that comprise the SC exhibit a depth dependent increase in cellular cohesion, due to heightened corneodesmosome density (Chapman and Walsh, 1990; Lin et al., 2012; Naoe et al., 2010). UVB irradiation has been proven to reduce the out-ofplane delamination energy of the basal layer cells in the SC by a greater amount than in the superficial layers (Biniek et al., 2012). This depth dependent correlation further supports the notion that corneodesmosome integrity plays a substantial role in defining the mechanical strength of the tissue, both in-plane and out-of-plane.

Future work regarding the scaling relationships established in this study should also be further tested. Although we cannot assert for certain why our scaling relationships exhibit an exponential behavior, exponential changes in skin composition and microstructure have been previously observed. Chronic exposure to UV has shown to exponentially increase DNA dimerization (Mitchell et al., 1999; Vink et al., 1991), ornithine decarboxylase activity (Hillebrand et al., 1990), and lipid peroxide levels (Iizawa et al., 1994) in mouse skin. This relationship could be further elicited by performing tests on full thickness ex vivo skin, in which the interaction between other skin components with UV can be interpreted. In addition, the validity of using absorbed energy and structural protein dispersion as a predictor of biomechanical photoaging should be assessed over a wider range of the electromagnetic spectrum and in deeper skin layers, perhaps through biomechanical testing and immunostaining of progressively thicker skin specimens that retain epidermal, then dermal tissue.

Conflict of interest

The authors state no conflict of interest.

Acknowledgements

This material is based upon work supported by the National Science Foundation under Grant No. 1653071. We would like to sincerely thank the reviewers for their suggestions and comments.

Appendix. A. Supplementary data

Supplementary data to this article can be found online at https://doi.org/10.1016/j.jmbbm.2019.103391.

References

Alonso, a, Meirelles, N.C., Yushmanov, V.E., Tabak, M., 1996. Water increases the fluidity of intercellular membranes of stratum corneum: correlation with water permeability, elastic, and electrical resistance properties. J. Invest. Dermatol. https://doi.org/10. 1111/1523-1747.ep12338682.

Amagai, M., Yamaguchi, T., Hanakawa, Y., Nishifuji, K., Sugai, M., Stanley, J.R., 2002. Staphylococcal exfoliative toxin B specifically cleaves desmoglein 1. J. Invest. Dermatol. https://doi.org/10.1046/j.1523-1747.2002.01751.x.

Arundel, A.V., Sterling, E.M., Biggin, J.H., Sterling, T.D., 1986. Indirect health effects of relative humidity in indoor environments. Environ. Health Perspect. https://doi.org/ 10.1289/ehp.8665351.

ASTM G173-03(2012), 2012. Standard tables for reference solar spectral irradiances: direct normal and hemispherical on 37* tilted surface. Am. Soc. Test. Mater. 1–21. https://doi.org/10.1520/G0173-03R12.

Besaratinia, A., Yoon, J. -i., Schroeder, C., Bradforth, S.E., Cockburn, M., Pfeifer, G.P., 2011. Wavelength dependence of ultraviolet radiation-induced DNA damage as determined by laser irradiation suggests that cyclobutane pyrimidine dimers are the principal DNA lesions produced by terrestrial sunlight. FASEB J. https://doi.org/10. 1096/fi.11-187336.

Biniek, K., Levi, K., Dauskardt, R.H., 2012. Solar UV radiation reduces the barrier function

- of human skin. Proc. Natl. Acad. Sci. 109, 17111–17116. https://doi.org/10.1073/pnas.1206851109.
- Böni, R., Schuster, C., Nehrhoff, B., Burg, G., 2002. Epidemiology of skin cancer. Neuroendocrinol. Lett. 23, 48–51. https://doi.org/10.1046/j.1365-2133.146.s61.2.x.
- Borgoño, C.A., Michael, I.P., Komatsu, N., Jayakumar, A., Kapadia, R., Clayman, G.L., Sotiropoulou, G., Diamandis, E.P., 2007. A potential role for multiple tissue kallikrein serine proteases in epidermal desquamation. J. Biol. Chem. https://doi.org/10. 1074/jbc.M607567200.
- Brem, R., Macpherson, P., Guven, M., Karran, P., 2017. Oxidative stress induced by UVA photoactivation of the tryptophan UVB photoproduct 6-formylindolo[3,2-b]carbazole (FICZ) inhibits nucleotide excision repair in human cells. Sci. Rep. https://doi.org/10.1038/s41598-017-04614-8.
- Bruls, W.A.G., Slaper, H., van Der Leun, J.C., Berrens, L., 1984. Transmission of human epidermis and stratum corneum as a function of thickness in the ultraviolet and visible wavelengths. Photochem. Photobiol. 40, 485–494. https://doi.org/10.1111/j. 1751-1097.1984.tb04622.x.
- Bruls, W.A.G., Van Der Leun, J.C., 1984. Forward scattering properties of human epidermal layers. Photochem. Photobiol. https://doi.org/10.1111/j.1751-1097.1984. tb04581 x
- Buckman, S., 1998. COX-2 expression is induced by UVB exposure in human skin: implications for the development of skin cancer. Carcinogenesis 19, 723–729. https://doi.org/10.1093/carcin/19.5.723.
- Chapman, S.J., Walsh, A., 1990. Desmosomes, corneosomes and desquamation. An ultrastructural study of adult pig epidermis. Arch. Dermatol. Res. https://doi.org/10.1007/BF00375724.
- Chen, A.C., Halliday, G.M., Damian, D.L., 2013. Non-melanoma skin cancer: carcinogenesis and chemoprevention. Pathology 45, 331–341. https://doi.org/10.1097/PAT.0b013e32835f515c.
- Cho, S., Shin, M.H., Kim, Y.K., Seo, J.-E., Lee, Y.M., Park, C.-H., Chung, J.H., 2009. Effects of infrared radiation and heat on human skin aging in vivo. J. Investig. Dermatol. Symp. Proc. 14, 15–19. https://doi.org/10.1038/jidsymp.2009.7.
- Cork, M.J., Robinson, D.A., Vasilopoulos, Y., Ferguson, A., Moustafa, M., MacGowan, A., Duff, G.W., Ward, S.J., Tazi-Ahnini, R., 2006. New perspectives on epidermal barrier dysfunction in atopic dermatitis: gene-environment interactions. J. Allergy Clin. Immunol. https://doi.org/10.1016/j.jaci.2006.04.042.
- D'Orazio, J., Jarrett, S., Amaro-Ortiz, A., Scott, T., 2013. UV radiation and the skin. Int. J. Mol. Sci. https://doi.org/10.3390/ijms140612222.
- Dai, A., 2006. Recent climatology, variability, and trends in global surface humidity. J. Clim. https://doi.org/10.1175/JCLI3816.1.
- de Gruijl, F.R., Van Kranen, H.J., Mullenders, L.H.F., 2001. UV-induced DNA damage, repair, mutations and oncogenic pathways in skin cancer. J. Photochem. Photobiol. B Biol. 63, 19–27. https://doi.org/10.1016/S1011-1344(01)00199-3.
- De Rie, M.A., Enomoto, D.N.H., De Vries, H.J.C., Bos, J.D., 2003. Evaluation of medium-dose UVA1 phototherapy in localized scleroderma with the cutometer and fast Fourier transform method. Dermatology 207, 298–301. https://doi.org/10.1159/000073093.
- Descargues, P., Draison, C., Bonnart, C., Kreft, M., Kishibe, M., Ishida-Yamamoto, A., Elias, P., Barrandon, Y., Zambruno, G., Sonnenberg, A., Hovnanian, A., 2005. Spink5-deficient mice mimic Netherton syndrome through degradation of desmoglein 1 by epidermal protease hyperactivity. Nat. Genet. https://doi.org/10.1038/ng1493.
- Diffey, B.L., 1983. A mathematical model for ultraviolet optics in skin. Phys. Med. Biol. 28, 647. https://doi.org/10.1088/0031-9155/28/6/005.
- Dixon, A.J., Dixon, B.F., 2004. Ultraviolet radiation from welding and possible risk of skin and ocular malignancy. Med. J. Aust. 181, 155–157. https://doi.org/10.5694/j.1326-5377.2004.tb06207.x [pii].
- Dong, K.K., Damaghi, N., Picart, S.D., Markova, N.G., Obayashi, K., Okano, Y., Masaki, H., Grether-Beck, S., Krutmann, J., Smiles, K.A., Yarosh, D.B., 2008. UV-induced DNA damage initiates release of MMP-1 in human skin. Exp. Dermatol. 17, 1037–1044. https://doi.org/10.1111/j.1600-0625.2008.00747.x.
- Eyre, R., Stanley, J., 1987. Human autoantibodies against a desmosomal protein complex with a calcium-sensitive epitope are characteristic of pemphigus foliaceus patients. J. Exp. Med. https://doi.org/10.1084/jem.165.6.1719.
- Fujita, H., Hirao, T., Takahashi, M., 2007. A simple and non-invasive visualization for assessment of carbonylated protein in the stratum corneum. Ski. Res. Technol. 13, 84–90. https://doi.org/10.1111/j.1600-0846.2007.00195.x.
- Gasperini, A.E., Sanchez, S., Doiron, A.L., Lyles, M., German, G.K., 2017. Non-ionising UV light increases the optical density of hygroscopic self assembled DNA crystal films. Sci. Rep. 7. https://doi.org/10.1038/s41598-017-06884-8.
- German, G.K., Pashkovski, E., Dufresne, E.R., 2013. Surfactant treatments influence drying mechanics in human stratum corneum. J. Biomech. 46, 2145–2151. https:// doi.org/10.1016/j.jbiomech.2013.07.003.
- Hillebrand, G.G., Winslow, M.S., Benzinger, M.J., Heitmeyer, D.A., Bissett, D.L., 1990. Acute and chronic ultraviolet radiation induction of epidermal ornithine decarboxylase activity in hairless mice. Cancer Res.
- Hirao, T., Takahashi, M., 2005. Carbonylation of cornified envelopes in the stratum corneum. FEBS Lett. 579, 6870–6874. https://doi.org/10.1016/j.febslet.2005.11. 032.
- Hoffmann, K., Kaspar, K., Altmeyer, P., Gambichler, T., 2000. UV transmission measurements of small skin specimens with special quartz cuvettes. Dermatology. https://doi.org/10.1159/000051543.
- Iizawa, O., Kato, T., Tagami, H., Akamatsu, H., Niwa, Y., 1994. Long-term follow-up study of changes in lipid peroxide levels and the activity of superoxide dismutase, catalase and glutathione peroxidase in mouse skin after acute and chronic UV irradiation. Arch. Dermatol. Res. https://doi.org/10.1007/BF00375843.
- Iwai, I., Hirao, T., 2008. Protein carbonyls damage the water-holding capacity of the stratum corneum. Skin Pharmacol. Physiol. 21, 269–273. https://doi.org/10.1159/

000148042

- Jiang, Y., Rabbi, M., Kim, M., Ke, C., Lee, W., Clark, R.L., Mieczkowski, P.A., Marszalek, P.E., 2009. UVA generates pyrimidine dimers in DNA directly. Biophys. J. 96, 1151–1158. https://doi.org/10.1016/j.bpj.2008.10.030.
- Johnson, J.L., Koetsier, J.L., Sirico, A., Agidi, A.T., Antonini, D., Missero, C., Green, K.J., 2014. The desmosomal protein desmoglein 1 aids recovery of epidermal differentiation after acute UV light exposure. J. Invest. Dermatol. https://doi.org/10. 1038/iid.2014.124.
- Jonca, N., Guerrin, M., Hadjiolova, K., Caubet, C., Gallinaro, H., Simon, M., Serre, G., 2002. Corneodesmosin, a component of epidermal corneocyte desmosomes, displays homophilic adhesive properties. J. Biol. Chem. https://doi.org/10.1074/jbc. M108432200
- Kitajima, Y., 2015. Implications of normal and disordered remodeling dynamics of corneodesmosomes in stratum corneum. Dermatol. Sin. https://doi.org/10.1016/j.dsi. 2015.03.009
- Kleinpenning, M.M., Smits, T., Boezeman, J., Van De Kerkhof, P.C.M., Evers, A.W.M., Gerritsen, M.J.P., 2009. Narrowband ultraviolet B therapy in psoriasis: randomized double-blind comparison of high-dose and low-dose irradiation regimens. Br. J. Dermatol. 161, 1351–1356. https://doi.org/10.1111/j.1365-2133.2009.09212.x.
- Kligman, A.M., Christophers, E., 1963. Preparation of isolated sheets of human stratum corneum. Arch. Dermatol. 88, 702–705. https://doi.org/10.1001/archderm.1963. 01590240026005
- Kollias, N., Baqer, A., 1984. An experimental study of the changes in pigmentation in human skin in vivo with visible and near infrared light. Photochem. Photobiol. 39, 651–659. https://doi.org/10.1111/j.1751-1097.1984.tb03905.x.
- Kolmel, K.F., Sennhenn, B., Giese, K., 1990. Investigation of skin by ultraviolet remittance spectroscopy. Br. J. Dermatol. https://doi.org/10.1111/j.1365-2133.1990. tb08267.x.
- Koutroupi, K.S., Barbenel, J.C., 1990. Mechanical and failure behaviour of the stratum corneum. J. Biomech. https://doi.org/10.1016/0021-9290(90)90018-X.
- Kreuter, A., Hyun, J., Stücker, M., Sommer, A., Altmeyer, P., Gambichler, T., 2006. A randomized controlled study of low-dose UVA1, medium-dose UVA1, and narrowband UVB phototherapy in the treatment of localized scleroderma. J. Am. Acad. Dermatol. 54, 440–447. https://doi.org/10.1016/j.jaad.2005.11.1063.
- Kroft, E.B.M., Berkhof, N.J.G., van de Kerkhof, P.C.M., Gerritsen, R.M.J.P., de Jong, E.M.G.J., 2008. Ultraviolet A phototherapy for sclerotic skin diseases: a systematic review. J. Am. Acad. Dermatol. https://doi.org/10.1016/j.jaad.2008.07.042.
- Kvam, E., Tyrrell, R.M., 1997. Induction of oxidative DNA base damage in human skin cells by UV and near visible radiation. Carcinogenesis 18, 2379–2384. https://doi. org/10.1093/carcin/18.12.2379.
- Langer, K., 1861. On the anatomy and physiology of the skin: the cleavability of the cutis. Br. J. Plast. Surg. 31, 3–8. https://doi.org/10.1016/0007-1226(78)90003-6.
- Lee, J.H., Roh, M.R., Lee, K.H., 2006. Effects of infrared radiation on skin photo-aging and pigmentation. Yonsei Med. J. 47, 485–490. https://doi.org/10.3349/ymj.2006.47.4.
- Lee, S.H., Matsushima, K., Miyamoto, K., Oe, T., 2016. UV irradiation-induced methionine oxidation in human skin keratins: mass spectrometry-based non-invasive proteomic analysis. J. Proteomics 133, 54–65. https://doi.org/10.1016/j.jprot.2015.11.026.
- Lin, T.K., Crumrine, D., Ackerman, L.D., Santiago, J.L., Roelandt, T., Uchida, Y., Hupe, M., Fabriàs, G., Abad, J.L., Rice, R.H., Elias, P.M., 2012. Cellular changes that accompany shedding of human corneocytes. J. Invest. Dermatol. https://doi.org/10.1038/jid. 2012.173.
- Liu, X., Cleary, J., German, G.K., 2016. The global mechanical properties and multi-scale failure mechanics of heterogeneous human stratum corneum. Acta Biomater. 43, 78–87. https://doi.org/10.1016/j.actbio.2016.07.028.
- Liu, X., German, G.K., 2015. The effects of barrier disruption and moisturization on the dynamic drying mechanics of human stratum corneum. J. Mech. Behav. Biomed. Mater. 49, 80–89. https://doi.org/10.1016/j.jmbbm.2015.04.017.
- Meechan, P.J., Wilson, C., 2006. Use of ultraviolet lights in biological safety cabinets: a contrarian view. Appl. Biosaf. 11, 222–227. https://doi.org/10.1177/ 153567600601100412.
- Meinhardt, M., Krebs, R., Anders, A., Heinrich, U., Tronnier, H., 2008. Wavelength-dependent penetration depths of ultraviolet radiation in human skin. J. Biomed. Opt. 13, 44030. https://doi.org/10.1117/1.2957970.
- Mitchell, D.L., Greinert, R., De Gruijl, F.R., Guikers, K.L.H., Breitbart, E.W., Byrom, M., Gallmeier, M.M., Lowery, M.G., Volkmer, B., 1999. Effects of chronic low-dose ultraviolet B radiation on DNA damage and repair in mouse skin. Cancer Res.
- Mizutani, T., Sumida, H., Sagawa, Y., Okano, Y., Masaki, H., 2016. Carbonylated proteins exposed to UVA and to blue light generate reactive oxygen species through a type I photosensitizing reaction. J. Dermatol. Sci. 84, 314–321. https://doi.org/10.1016/j. idermsci.2016.09.016.
- Moan, J., Porojnicu, A.C., Dahlback, A., Setlow, R.B., 2008. Addressing the health benefits and risks, involving vitamin D or skin cancer, of increased sun exposure. Proc. Natl. Acad. Sci. U. S. A. 105, 668–673. https://doi.org/10.1073/pnas.0710615105.
- Naoe, Y., Hata, T., Tanigawa, K., Kimura, H., Masunaga, T., 2010. Bidimensional analysis of desmoglein 1 distribution on the outermost corneocytes provides the structural and functional information of the stratum corneum. J. Dermatol. Sci. https://doi. org/10.1016/j.jdermsci.2009.12.014.
- Ní Annaidh, A., Bruyère, K., Destrade, M., Gilchrist, M.D., Otténio, M., 2012. Characterization of the anisotropic mechanical properties of excised human skin. J. Mech. Behav. Biomed. Mater. 5, 139–148. https://doi.org/10.1016/j.jmbbm.2011. 08.016.
- Nin, M., Katoh, N., Kokura, S., Handa, O., Yoshikawa, T., Kishimoto, S., 2009. Dichotomous effect of ultraviolet B on the expression of corneodesmosomal enzymes in human epidermal keratinocytes. J. Dermatol. Sci. https://doi.org/10.1016/j.

jdermsci.2008.11.004.

- Nishimori, Y., Edwards, C., Pearse, A., Matsumoto, K., Kawai, M., Marks, R., 2001. Degenerative alterations of dermal collagen fiber bundles in photodamaged human skin and UV-irradiated hairless mouse skin: possible effect on decreasing skin mechanical properties and appearance of wrinkles. J. Invest. Dermatol. 117, 1458–1463. https://doi.org/10.1038/jid.2001.2.
- Oba, A., Edwards, C., 2006. Relationships between changes in mechanical properties of the skin, wrinkling, and destruction of dermal collagen fiber bundles caused by photoaging. Ski. Res. Technol. 12, 283–288. https://doi.org/10.1111/j.0909-752X. 2006.00154.x.
- Oyama, Z., Naoe, Y., Kimura, H., Masunaga, T., Seishima, M., Aoyama, Y., Kitajima, Y., 2010. New non-invasive method for evaluation of the stratum corneum structure in diseases with abnormal keratinization by immunofluorescence microscopy of desmoglein 1 distribution in tape-stripped samples. J. Dermatol. https://doi.org/10.1111/j.1346-8138.2010.00875.x.
- Panich, U., Sittithumcharee, G., Rathviboon, N., Jirawatnotai, S., 2016. Ultraviolet radiation-induced skin aging: the role of DNA damage and oxidative stress in epidermal stem cell damage mediated skin aging. Stem Cell. Int. https://doi.org/10.1155/2016/7370642
- Papir, Y., Hsu, K., Wildnauer, R.H., Hsh, K., Wildnauer, R.H., Hsu, K., Wildnauer, R.H., 1975. The mechanical properties of stratum corneum: I. The effect of water and ambient temperature on the tensile properties of newborn rat stratum corneum. Biochim. Biophys. Acta 399, 170–180. https://doi.org/10.1016/0304-4165(75) 90223-8
- Pfeifer, G.P., 1997. Formation and processing of UV photoproducts: effects of DNA sequence and chromatin environment. Photochem. Photobiol. https://doi.org/10.1111/i.1751-1097.1997.tb08560.x.
- Pfeifer, G.P., Besaratinia, A., 2012. UV wavelength-dependent DNA damage and human non-melanoma and melanoma skin cancer. Photochem. Photobiol. Sci. https://doi. org/10.1039/c1pp05144j.
- Rawlings, A., Sabin, R., Harding, C., Watkinson, A., Banks, J., Ackerman, C., 1995. The effect of glycerol and humidity on desmosome degradation in stratum corneum. Arch. Dermatol. Res. https://doi.org/10.1007/BF00373429.
- Reynolds, N.J., Franklin, V., Gray, J.C., Diffey, B.L., Farr, P.M., 2001. Narrow-band ultraviolet B and broad-band ultraviolet A phototherapy in adult atopic eczema: a randomised controlled trial. Lancet 357, 2012–2016. https://doi.org/10.1016/S0140-6736(00)05114-X.
- Sander, C.S., Chang, H., Salzmann, S., Müller, C.S.L., Ekanayake-Mudiyanselage, S., Elsner, P., Thiele, J.J., 2002. Photoaging is associated with protein oxidation in human skin in vivo. J. Invest. Dermatol. 118, 618–625. https://doi.org/10.1046/j. 1523-1747.2002.01708 x.
- Schuch, A.P., Moreno, N.C., Schuch, N.J., Menck, C.F.M., Garcia, C.C.M., 2017. Sunlight damage to cellular DNA: focus on oxidatively generated lesions. Free Radic. Biol. Med. https://doi.org/10.1016/j.freeradbiomed.2017.01.029.
- Silva, C.L., Topgaard, D., Kocherbitov, V., Sousa, J.J.S., Pais, A.A.C.C., Sparr, E., 2007. Stratum corneum hydration: phase transformations and mobility in stratum corneum, extracted lipids and isolated corneocytes. Biochim. Biophys. Acta Biomembr. https:// doi.org/10.1016/j.bbamem.2007.05.028.
- Tadokoro, T., Kobayashi, N., Zmudzka, B.Z., Ito, S., Wakamatsu, K., Yamaguchi, Y., Korossy, K.S., Miller, S.A., Beer, J.Z., Hearing, V.J., 2003. UV-induced DNA damage and melanin content in human skin differing in racial/ethnic origin. FASEB J. 17, 1177–1179. https://doi.org/10.1096/fj.02-0865fje.
- Takahashi, M., Kawasaki, K., Tanaka, M., Ohta, S., Tsuda, Y., 1981. The mechanism of stratum corneum plasticization with water. In: Bioengineering and the Skin. Springer,

- pp. 67-73. https://doi.org/10.1007/978-94-009-7310-7_8.
- Thiele, J.J., Hsieh, S.N., Briviba, K., Sies, H., 1999. Protein oxidation in human stratum corneum: susceptibility of keratins to oxidation in vitro and presence of a keratin oxidation gradient in vivo. J. Invest. Dermatol. 113, 335–339. https://doi.org/10. 1046/i.1523-1747.1999.00693.x.
- Tjioe, M., Gerritsen, M.J.P., Juhlin, L., Van De Kerkhof, P.C.M., 2002. Treatment of vitiligo vulgaris with narrow band UVB (311 nm) for one year and the effect of addition of folic acid and vitamin B12. Acta Derm. Venereol. 82, 369–372. https://doi.org/10.1080/000155502320624113.
- U.S. Department of Health and Human Services, 2000. Report on Carcinogens Background Document for Ultraviolet (UV) Radiation.
- Valley, S.L., 1965. Handbook of Geophysics and Space Environments. Air Force Cambridge research labs hanscom AFB MA. https://doi.org/10.1063/1.3047784.
- Vink, A.A., Berg, R.J.W., de Gruijl, F.R., Roza, L., Baan, R.A., 1991. Induction, repair and accumulation of thymin dimers in the skin of UV-b-irradiated hairless mice. Carcinogenesis. https://doi.org/10.1093/carcin/12.5.861.
- Vyumvuhore, R., Tfayli, A., Duplan, H., Delalleau, A., Manfait, M., Baiilet-Guffroy, A., 2013. Effects of atmospheric relative humidity on Stratum Corneum structure at the molecular level: ex vivo Raman spectroscopy analysis. Analyst. https://doi.org/10.1039/c3an00716b.
- Walkley, K., 1972. Bound water in stratium corneum measured by differential scanning calorimetry. J. Invest. Dermatol. https://doi.org/10.1111/1523-1747.ep12627251.
- Warner, R.R., Stone, K.J., Boissy, Y.L., 2003. Hydration disrupts human stratum corneum ultrastructure. J. Invest. Dermatol. 120, 275–284. https://doi.org/10.1046/j.1523-1747.2003.12046.x.
- Wildnauer, R.H., Bothwell, J.W., Douglass, A.B., 1971. Stratum corneum biomechanical properties I. Influence of relative humidity on normal and extracted human stratum corneum. J. Invest. Dermatol. 56, 72–78. https://doi.org/10.1111/1523-1747. en1299018
- World Health Organization, International Programme on Chemical Safety, 1994.

 Ultraviolet Radiation: an Authoritative Scientific Review of Environmental and
 Health Effects of UV, with Reference to Global Ozone Layer Depletion. Environmental
 health criteria.
- Wu, K.S., van Osdol, W.W., Dauskardt, R.H., 2006. Mechanical Properties of Human Stratum Corneum: Effects of Temperature, Hydration, and Chemical Treatment. Biomaterials. https://doi.org/10.1016/j.biomaterials.2005.06.019.
- Yamasaki, K., Di Nardo, A., Bardan, A., Murakami, M., Ohtake, T., Coda, A., Dorschner, R.A., Bonnart, C., Descargues, P., Hovnanian, A., Morhenn, V.B., Gallo, R.L., 2007. Increased serine protease activity and cathelicidin promotes skin inflammation in rosacea. Nat. Med. https://doi.org/10.1038/nm1616.
- Yashar, S.S., Gielczyk, R., Scherschun, L., Lim, H.W., 2003. Narrow-band ultraviolet B treatment for vitiligo, pruritus, and inflammatory dermatoses. Photodermatol. Photoimmunol. Photomed. 19, 164–168. https://doi.org/10.1034/j.1600-0781. 2003.00039.x.
- Yokouchi, M., Atsugi, T., Van Logtestijn, M., Tanaka, R.J., Kajimura, M., Suematsu, M., Furuse, M., Amagai, M., Kubo, A., 2016. Epidermal cell turnover across tight junctions based on Kelvin's tetrakaidecahedron cell shape. Elife 5, e19593. https://doi.org/10.7554/elife.19593.001.
- Zhang, M., Qureshi, A.A., Geller, A.C., Frazier, L., Hunter, D.J., Han, J., 2012. Use of tanning beds and incidence of skin cancer. J. Clin. Oncol. 30, 1588–1593. https://doi. org/10.1200/JCO.2011.39.3652.
- Ziegler, A., Jonason, A.S., Leffellt, D.J., Simon, J.A., Sharma, H.W., Kimmelman, J., Remington, L., Jacks, T., Brash, D.E., 1994. Sunburn and p53 in the onset of skin cancer. Nature 372, 773–776. https://doi.org/10.1038/372773a0.